atmosphere

MDPI

Article

Trends in Precipitation and Air Temperature Extremes and Their Relationship with Sea Surface Temperature in the Brazilian Midwest

Luiz Octávio F. dos Santos [1], Nadja G. Machado [2], Marcelo S. Biudes [3,*], Hatim M. E. Geli [4], Carlos Alexandre S. Querino [5], Anderson L. Ruhoff [6], Israel O. Ivo [1] and Névio Lotufo Neto [1]

1 Graduate Program in Environmental Physics, Institute of Physics, Federal University of Mato Grosso, 2367, Av. Fernando Corrêa da Costa, Cuiabá 78.060-900, MT, Brazil
2 Federal Institute of Mato Grosso, Av. Juliano da Costa Marques, Cuiabá 78.050-560, MT, Brazil
3 Institute of Physics, Federal University of Mato Grosso, 2367, Av. Fernando Corrêa da Costa, Cuiabá 78.060-900, MT, Brazil
4 New Mexico Water Resources Institute and Department of Animal and Range Sciences, New Mexico State University, Las Cruces, NM 88003, USA
5 Institute of Agriculture and Environment Education, Federal University of Amazonas, 786, Rua 29 de Agosto, Humaitá 69.800-000, AM, Brazil
6 Institute of Hydraulic Research, Federal University of Rio Grande do Sul, 9500, Av. Bento Gonçalves, Porto Alegre 91.501-970, RS, Brazil
* Correspondence: marcelo@fisica.ufmt.br; Tel.: +55-65-99606-8893

Abstract: The Brazilian Midwest has significant spatiotemporal variability in terms of precipitation and air temperature, making it more vulnerable to the occurrence of extreme weather events. The objective of this study is to characterize the trend of extreme climatic events regarding precipitation and air temperature in the Brazilian Midwest, and to analyze their relationship with Pacific and Atlantic Sea Surface Temperature anomalies (SSTAs). We used daily precipitation and air temperature data measured at 24 conventional weather stations. Pacific and Atlantic SSTA data were obtained from the Climate Prediction Center. The frequency of hot extremes had increased, while that of cold extremes had decreased significantly, thus highlighting the consistent warming across the Brazilian Midwest. The precipitation extremes had greater variability than the temperature extremes. Precipitation intensity increased in Amazonia, with no change in annual precipitation volume. The precipitation extremes in the Brazilian Savanna, Pantanal, and the Atlantic Forest did not have a well-defined pattern but indicated a trend towards a decrease in days with intense precipitation events. In general, the Equatorial Pacific and Atlantic Ocean (TNAI and TSAI) SSTAs were negatively correlated with precipitation extreme indices and positively correlated with air temperature extreme indices in the Amazon. However, the North Atlantic SSTAs were positively correlated with precipitation and air temperature extreme indices in the Brazilian Savanna and Pantanal. In addition, the Pacific SSTAs were positively correlated with precipitation intensity in the Atlantic Forest. Thus, the variability of the trends of precipitation and air temperature extreme indices in the Brazilian Midwest was observed, and it was surmised that this measure was significantly related to Pacific and Atlantic SSTAs.

Keywords: South America; SST anomalies; precipitation; air temperature; climate variability

Citation: dos Santos, L.O.F.; Machado, N.G.; Biudes, M.S.; Geli, H.M.E.; Querino, C.A.S.; Ruhoff, A.L.; Ivo, I.O.; Lotufo Neto, N. Trends in Precipitation and Air Temperature Extremes and Their Relationship with Sea Surface Temperature in the Brazilian Midwest. *Atmosphere* **2023**, *14*, 426. https://doi.org/10.3390/atmos14030426

Academic Editors: Mingzhong Xiao and Futing Wu

Received: 13 January 2023
Revised: 16 February 2023
Accepted: 16 February 2023
Published: 21 February 2023

1. Introduction

The Brazilian Midwest contains diverse, natural tropical ecosystems, which predominantly consist of the Amazon, Brazilian Savanna, Pantanal, and Atlantic Forest biomes, and is characterized by complex climate variability [1]. These systems provide ecological resources and services, as well as valuable benefits to human systems (e.g., socioeconomics and livelihoods) regionally [2]. The suitability of this region's climate makes it one of the

largest producers of meat, soybeans, cotton, corn, sugarcane, and rice in Brazil [3]. Unfortunately, these systems have been, and will continue to be, exposed and thus vulnerable to a wide range of hazards that emerge from changes in the conditions of the physical climate system [2]. These changes can be characterized by extreme climate events (e.g., heat waves, cold waves, dry spells, etc.) corresponding to specific essential climate variables [4], including precipitation and temperature. The occurrence of these extreme events has been more frequent and intense/severe in recent years, which has spurred the need to better understand their spatial and temporal variability and characteristics (duration, frequency, and severity) since such events can lead to wildfires, floods, drought, the loss of property, the loss of infrastructure, human health impacts, severe decreases in crop and animal production, and reduced economic stability [5–7], thus necessitating a better understanding of the region's climate extreme trends to plan adaptation and mitigation strategies.

The assessment of climate extremes has been the focus of many regional and global studies as they can directly and indirectly be related to the vulnerability of natural and human systems to climate impacts. Climate extremes, as defined by the IPCC, are events concerning the occurrence of unusual values/magnitude of observed essential climate variables [2], and they are related to Climatic Impact-Drivers (CID) that evaluate climate conditions that affect a component of society or ecosystems. Changes in these extremes (magnitude and frequency), which can be computed using several indices that can allow for the characterization of their variability and trends [7], can directly lead to changes in impact [8]. Thus, studying the variability of these extremes can provide guidance for the management of natural disasters [9]. Some tools have been developed to efficiently calculate major climate extreme indicators, including the ClimDex, which was developed as an outcome of the recommendations made by the World Climate Research Program (WCRP) of the World Meteorological Organization (WMO) [10].

Large-scale circulation patterns modify weather patterns and are related to the gradients of Sea Surface Temperature (SST) anomalies over the Equatorial Pacific (El Niño Southern Oscillation—ENSO) and Atlantic (Atlantic Dipole) oceans [11,12]. SST is a causative factor of global climate variation, and ocean–atmosphere interactions interfere with atmospheric circulation patterns on a global scale, thus causing changes in temperature and precipitation over continents [13]. Therefore, the oceans play an extremely important role in the planet's climate [14]. Among the events caused by the variation in the Pacific SST, El Niño (warm phase) and La Niña (cold phase) are the best known for causing fluctuations in atmospheric pressure at sea level and providing changes in atmospheric circulation, which favor the intensification of extreme drought and flood events [13]. On the other hand, the Atlantic Dipole is an SST anomaly in the North and South sectors of the Atlantic Ocean, which has two phases (positive and negative). The positive phase presents positive SST anomalies in the North Atlantic sector and negative in the South sector, and an inversion in the pattern of anomalies occurs in the negative phase [15].

Several studies have indicated the existence of climate change based on trends in climate extreme indices in South America [16–21]; however, few of them have considered the regional variability in the Brazilian Midwest. In addition, these studies used monthly and annual averages across the region and disregarded daily data [7] as well as large-scale phenomena such as SST anomalies. Thus, this study has been motivated by the lack of characterization of the precipitation and temperature extreme indices of this region. The goal of this study is to provide a clear depiction of the observed physical climatic changes in the region that can inform (or be used for) hazard, vulnerability, and adaptation assessment studies for the Brazilian Midwest that focus on periods since 1970. The objective of this study was to (i) evaluate climate extreme indices based on temperature and precipitation (as identified by the IPCC report [2]), (ii) identify the historical changes and trends of these climate extreme indices, and (iii) assess the ability of the SST of the Pacific and Atlantic oceans to depict/predict the changes in these indices. The results of this study can be used by decision-makers and resource managers for developing practices and policies that

can enhance mitigation and adaption efforts in the Brazilian Midwest, South America in general, and elsewhere.

2. Materials and Methods

2.1. Study Area

The Brazilian Midwest is in the central region of South America (Figure 1), comprising the states of Mato Grosso (MT), Mato Grosso do Sul (MS), Goiás (GO), and Distrito Federal (DF). This region is approximately 135.4 × 10^6 km^2 in area; is at an altitude from 47 to 1674 m; comprises the Brazilian Savanna (57%), Amazon (30%), Pantanal (9%), and Atlantic Forest (4%) biomes; and the climate has temperature and precipitation gradients that lead to the formation of the following climatic zones: Aw (tropical with dry winter), Am (tropical humid), Cwa (subtropical with dry winter and hot summer), and Cfa (subtropical with hot summer) according to the Köppen–Geiger classification [22].

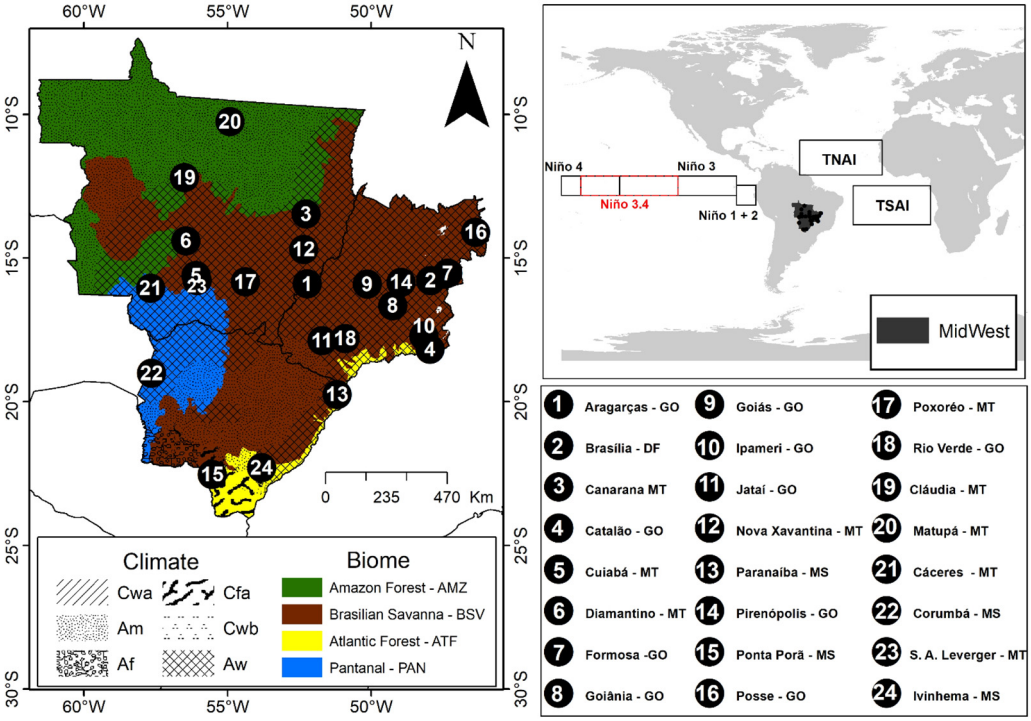

Figure 1. Location of Conventional Weather Stations, climates, and biomes of the Brazilian Midwest, and areas of operation of ENSO (Niño 1 + 2, Niño 3, Niño 3.4 and Niño 4) in the Equatorial Pacific, and Atlantic Dipole (TNAI and TSAI) in the Tropical Atlantic.

2.2. Data

2.2.1. Precipitation and Temperature Data

Daily precipitation and maximum and minimum air temperature data for the 1979 to 2019 period were obtained from 24 conventional weather stations from the Meteorological Database for Teaching and Research (BDMEP) [23] of the Brazilian National Institute of Meteorology (INMET) (Table 1). All conventional weather stations with available data from 1979 to 2019 were used in this study. The inclusion of areas with limited meteorological data from conventional weather stations did not affect the quality of the findings in this study, since the World Meteorological Organization (WMO) has established that the horizontal interval between stations should not exceed 250–300 km in regions with a sparse distribution of stations [24].

Table 1. Characterization of the conventional meteorological stations, WMO codes, ID, sites, biomes, climates, latitudes, longitudes, and elevations in the Brazilian Midwest.

WMO Code	ID	Sites	Biome	Climate	Latitude (degree)	Longitude (degree)	Elevation (m)
83368	1	Aragarças—GO	Brazilian Savanna	Aw	−15.9	−52.23	345
83377	2	Brasília—DF	Brazilian Savanna	Cwa	−15.78	−47.93	1159.54
83270	3	Canarana—MT	Brazilian Savanna	Aw	−13.47	−52.27	430
83526	4	Catalão—GO	Brazilian Savanna	Cwa	−18.18	−47.95	840.47
83361	5	Cuiabá—MT	Brazilian Savanna	Aw	−15.61	−56.1	145
83309	6	Diamantino—MT	Brazilian Savanna	Aw	−14.4	−56.45	286.3
83379	7	Formosa—GO	Brazilian Savanna	Aw	−15.53	−47.33	935.19
83423	8	Goiânia—GO	Brazilian Savanna	Aw	−16.66	−49.25	741.48
83374	9	Goiás—GO	Brazilian Savanna	Aw	−15.91	−50.13	512.22
83522	10	Ipameri—GO	Brazilian Savanna	Aw	−17.71	−48.16	772.99
83464	11	Jataí—GO	Brazilian Savanna	Aw	−17.88	−51.71	662.86
83319	12	Nova Xavantina—MT	Brazilian Savanna	Aw	−14.7	−52.35	316
83565	13	Paranaíba—MS	Brazilian Savanna	Aw	−19.75	−51.18	331.25
83376	14	Pirenópolis—GO	Brazilian Savanna	Aw	−15.85	−48.96	740
83702	15	Ponta Porã—MS	Brazilian Savanna	Cfa	−22.53	−55.53	650
83332	16	Posse—GO	Brazilian Savanna	Aw	−14.1	−46.36	825.64
83358	17	Poxoréo—MT	Brazilian Savanna	Aw	−15.83	−54.38	450
83470	18	Rio Verde—GO	Brazilian Savanna	Aw	−17.8	−50.91	774.62
83264	19	Cláudia—MT	Amazon Forest	Aw	−12.2	−56.5	415
83214	20	Matupá—MT	Amazon Forest	Am	−10.25	−54.91	285
83405	21	Cáceres—MT	Pantanal	Aw	−16.05	−57.68	118
83552	22	Corumbá—MS	Pantanal	Aw	−19.01	−57.65	130
83364	23	Sto Ant. de Leverger—MT	Pantanal	Aw	−15.78	−56.06	140
83704	24	Ivinhema—MS	Atlantic Forest	Aw	−22.3	−53.81	369.2

2.2.2. SST Anomalies Indices

Six different SST-based anomalies have been used in this study. The values of these anomalies were obtained from the Climate Prediction Center (CPC) of the National Oceanic and Atmospheric Administration (NOAA). The selected SST-based indices include the Niño 1 + 2 (0–10S, 90W–80W), Niño 3 (5N–5S, 150W–90W), Niño 3.4 (5N–5S, 170W–120W), Niño 4 (5N–5S, 160E–150W), ONI (5N–5S, 170W–120W), TNAI (5.5N–23.5N, 15W–57.5W), and TSAI (Ecuador-20S, 10E–30W) (Figure 1). The Oceanic Niño Index (ONI) uses the Niño 3.4 region and is calculated from the 3-month moving average of SST anomalies from NOAA Extended Reconstructed Sea Surface Temperature (SST) V5 [25].

2.3. Climate Extreme Indices

This study evaluated the interannual variability and long-term trends in extreme events' characteristics in terms of magnitude/severity, duration, and frequency by focusing on extreme warm and cold (i.e., temperature-based extremes) as well as extreme wet and dry (i.e., precipitation-based extremes) events from 1979 to 2019. Changes in the frequency of occurrence of heavy precipitation events that exceeded daily amounts of 10, 20, and 50 mm were assessed, as well as maximum amounts that occurred in 1- or 5-day events and those that exceeded 95th or 99th percentiles. Other changes in precipitation events that have been considered are related to the persistence of these events. In other words, assessment of consecutive wet or dry periods can allow for the determination of whether precipitation events have been occurring in short periods as well as the periods between them. Assessment of extremes often involves the evaluation of the tails of the distributions using non-parametric approaches to identify the extreme events.

Similarly, the study evaluated the duration, frequency, and severity of temperature extremes in terms of maximum and minimum day and night temperature and the consecutive

number of days with warm (temperature exceeds the 90th percentile) or cold (temperature is less than the 10th percentile) spells based on the 1979–2019 period.

Following the recommendation of the World Climate Research Group (WCRP) [26], this study selected and calculated a number of indices. This study also utilized a tool that was jointly developed by the WCRP and the Canadian Meteorological Service (CMS) research departments [27] to calculate these indices. This tool is referred to as RClimDex (version 1.0), and it is based on R language. The RClimDex calculates 27 climate extreme indices derived from temperature and precipitation based on Climate Change Detection Monitoring and Indices (ETCCDMI). In this study, we have evaluated 22 indices most suitable for the climatology of the Midwest region of Brazil. Specifically, the study evaluated 11 indices derived from precipitation and 11 from air temperature, as listed in Table 2. More details about how these indices were calculated can be found in [28].

Table 2. Description of precipitation and air temperature climate extreme indices for the Brazilian Midwest. Tmax: Maximum Temperature; Tmin: Minimum Temperature; PRCP: Daily Precipitation.

Variable	Group	Index	ID	Definition	Units
Precipitation	Threshold	Number of heavy precipitation days	R10mm	Annual count of days when PRCP $\geq$ 10 mm	days
		Number of very heavy precipitation days	R20mm	Annual count of days when PRCP $\geq$ 20 mm	days
		Number of days with precipitation above 50 mm	R50mm	Annual count of days when PRCP $\geq$ 50 mm	days
	Absolute	Maximum 1-day precipitation amount	Rx1day	Annual maximum 1 day precipitation	mm
		Maximum 5-day precipitation amount	Rx5day	Annual maximum 5-day precipitation	mm
	Other	Annual total wet day precipitation	PRCPTOT	Annual total precipitation in wet days PRCP $\geq$ 1 mm	mm
		Simple daily Intensity Index	SDII	Annual total precipitation divided by the number of wet days—PRCP $\geq$ 1 mm	mm/day
	Percentile	Precipitation on very wet days	R95p	Annual total precipitation when PRCP > 95th percentile	mm
		Precipitation on extremely wet days	R99p	Annual total precipitation when PRCP > 99th percentile	mm
	Duration	Consecutive wet days	CWD	Maximum number of consecutive days when PRCP $\geq$ 1 mm	days
		Consecutive dry days	CDD	Maximum number of consecutive days when PRCP < 1 mm	days
Air temperature	Absolute	Warmest Day	TXx	Annual Maximum value of daily maximum temperature	°C
		Warmest Night	TNx	Annual Maximum value of daily min temperature	°C
		Coldest Day	TXn	Annual Minimum value of daily maximum temperature	°C
		Coldest Night	TNn	Annual Minimum value of daily min temperature	°C
		Diurnal Temperature Range	DTR	Daily Tmax—Daily Tmin	°C
	Duration	Warm spell duration	WDSI	Annual count of days with a least 6 consecutive days when Tmax > 90th percentile	days
		Cold spell duration	CSDI	Annual count of days with a least 6 consecutive days when Tmin < 10th percentile	days
	Percentile	Warm Days	TX90p	% of days when Tmax is > 90th percentile	%
		Warm Nights	TN90p	% of days when Tmin is > 90th percentile	%
		Cool Days	TX10p	% of days when Tmax is < 90th percentile	%
		Cool Nights	TN10p	% of days when Tmin is < 90th percentile	%

2.4. Statistical Analysis

Quality control of climate data was performed to identify missing data, manual typing errors, and outliers [27,29]. Negative daily precipitation was removed, and daily maximum and minimum temperatures were defined as absent when the daily maximum temperature was lower than the daily minimum temperature. Outliers in daily maximum and minimum temperature were also identified and set to absent when they were 4 × std (standard deviations) from the climatological normal. Quality control processes were conducted using the RClimdex tool.

Trends in climate extreme indices are usually calculated by the non-parametric Mann–Kendall (MK) test [30]. A positive MK test value indicates a positive trend, while a negative value indicates a negative trend. The assumption of the MK test is that the time series has independent and randomly distributed data, which was verified using the Autocorrelation Function (ACF). As the dataset is autocorrelated, the magnitude of trends in climate extreme indices was calculated using the Theil–Sen method, which is insensitive to outliers and can be significantly more accurate than simple linear regression for distorted and heteroscedastic data [31], and the significance of these trends' magnitude was calculated by the Modified Mann–Kendall (MMK) test [32].

The Kernel Probability Density Function (PDF) was used to identify probable changes in the mean, variability, and asymmetry of the data distributions in relation to the patterns of precipitation and air temperature climate extreme indices. To assess the changes in the PDF, the data were split into 4 decades: 1979–1989, 1990–1999, 2000–2009, and 2010–2019. Kernel PDF is a statistical analysis technique used to model the probability distribution of a random, usually continuous variable, using a smooth function (known as the kernel) to approximate the shape of the probability distribution. The aim of the Kernel PDF is to produce a non-parametric estimate of the probability distribution, without assuming a specific shape for the underlying distribution [33]. Moreover, Pearson's correlation and its significance according to the Student's t test were used to assess the relationship between the precipitation and air temperature extreme indices with the SST anomalies [11]. The effective degrees of freedom (EDOF) of correlations between variables of different characteristics can be estimated from autoregressive properties in both databases [34,35]. We estimated the EDOF using the method proposed by [36].

3. Results

3.1. Precipitation Extremes

3.1.1. Spatiotemporal Variability

The number of days with heavy precipitation (R10mm) had a negative trend in 25% of the weather stations, with the highest negative trend in Goiás (ID 9; 0.47 day year^{-1}) (Table 3 and Figure 2A), while the rest of the stations had no change over the last 40 years. The negative trend in R10mm was mainly in the western part of the Midwest. The number of days with very heavy precipitation (R20mm) showed mostly no change across the study region, except for four stations: two stations had a positive trend and two had a negative trend (Figure 2B). The number of days with precipitation above 50 mm (R50mm) had a positive trend in 25% of the sites, with the highest at Matupá (ID 20; 0.29 day year^{-1}) (Figure 2C).

The maximum 1-day precipitation amount (Rx1day) index had a positive trend in 17% of the sites, with the highest at Matupá (ID 20; 2.02 mm year^{-1}) (Figure 2D). However, the maximum 5-day precipitation amount (Rx5day) had a mostly positive trend (Figure 2E). For example, Rx5day had positive trends in the North, Central, and South regions of the Midwest and negative trends in the East. The highest significant positive trend of Rx5day was at Matupá (ID 20; 2.99 mm year^{-1}), which is in the central Midwest, and the highest negative trend was at Goiás (ID 9; −2.00 mm year^{-1}) in the western of the Midwest. The total annual amount of precipitation on wet days (PRCPTOT) had a positive trend only at Diamantino (ID 6; 6.93 mm year^{-1}), and most negative trends were observed in the east

part of the Midwest, with the highest values observed at Goiás (ID 9; −17.20 mm year^{-1}) (Figure 2F).

Table 3. The percentage of stations with significant positive or negative trends and no trend of the precipitation and air temperature climate extreme indices according to the Mann–Kendall test for the Midwest region of Brazil from 1979 to 2019.

Index		Units	% of Stations with Positive Trend	% of Stations with Negative Trend	% of Stations with No Trend
Precipitation	R10mm	days	0	25	75
	R20mm	days	8.3	8.3	83.3
	R50mm	days	25	0	75.1
	RX1day	mm	16.7	0	83.3
	RX5day	mm	20.8	12.5	66.6
	PRCPTOT	mm	4.2	16.7	79.1
	SDII	mm/day	50	4.2	45.8
	R95p	mm	29.2	0	70.8
	R99p	mm	25	4.2	70.9
	CWD	days	0	37.5	62.6
	CDD	days	12.5	0	87.5
Air temperature	TXx	°C	91.7	0	8.3
	TNx	°C	45.8	0	54.2
	TXn	°C	54.2	0	45.9
	TNn	°C	50	0	50
	DTR	°C	62.5	0	37.5
	WSDI	days	20.8	0	79.1
	CSDI	days	0	0	100
	TX90p	%	95.8	0	4.2
	TN90p	%	62.5	0	37.5
	TX10p	%	0	79.2	20.8
	TN10p	%	0	62.5	37.5

Over the past 40 years, the precipitation intensity has increased across the Brazilian Midwest as indicated by the Simple Daily Intensity Index (SDII), the precipitation on very wet days (R95p) index, and the precipitation on extremely wet days (R99p) index (Table 3). The SDII had a positive trend in 50% of the sites, and a negative trend only in Goiás (ID 9; −0.08 mm year^{-1}). The highest significant positive trend of SDII was in Matupá (ID 20; 0.20 mm year^{-1}) (Figure 2G). The R95p and R99p indices had a positive trend in 29% of the sites (Figure 2H,I), in which the highest positive trends were in Matupá (ID 20; R95p = 19.42 mm year^{-1} and R99p = 7.28 mm year^{-1}) and the only negative trend of R99p occurred in Catalão (ID 4; −0.82 mm year^{-1}).

Another indicator of the sporadic occurrence of precipitation is based on the observed negative trends in the Consecutive Wet Days (CWD) and positive trends in the Consecutive Dry Days (CDD) indices. The CWD index had a negative trend in 38% of the sites distributed in a West–East direction (Figure 2J), wherein the highest negative trend of the CWD occurred in Nova Xavantina (ID 12; −0.39 day year^{-1}) and the lowest in Brasília (ID 2; −0.07 day year^{-1}). On the other hand, the CDD had a positive trend in ~13% of the sites (Figure 2K), wherein the highest significant positive trend of the CDD occurred in Canarana (ID 3; 1.13 day year^{-1}) and the lowest one in Corumbá (ID 22; 0.54 day year^{-1}).

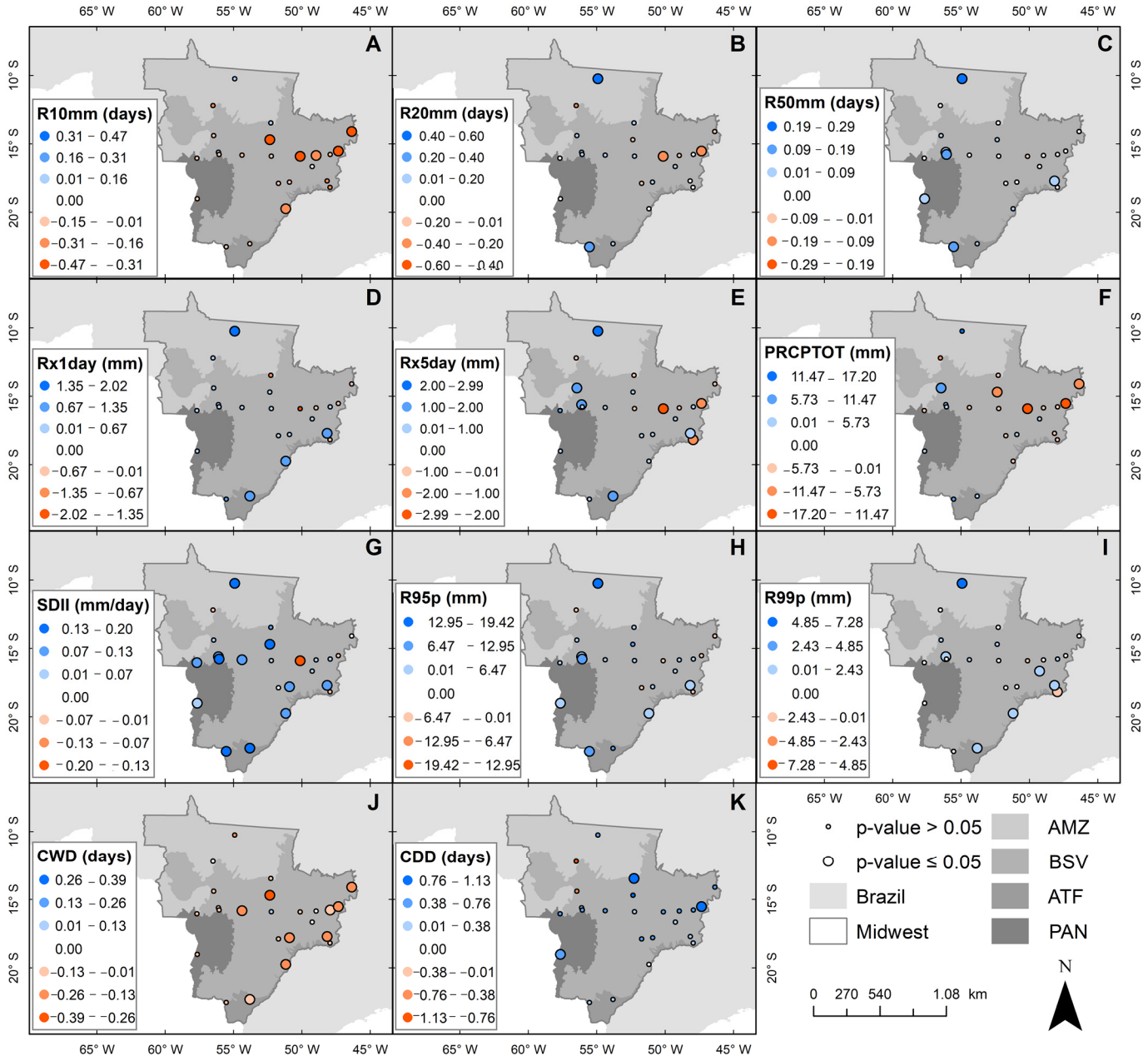

Figure 2. Spatial distribution of trends regarding number of heavy precipitation days (R10mm) (**A**), number of very heavy precipitation days (R20mm) (**B**), number of days above 50 mm (R50mm) (**C**), maximum 1-day precipitation amount (Rx1day) (**D**), maximum 5-day precipitation amount (Rx5day) (**E**), annual total wet day precipitation (PRCPTOT) (**F**), simple daily intensity index (SDII) (**G**), precipitation on very wet days (R95p) (**H**), precipitation on extremely wet days (R99p) (**I**), consecutive wet days (CWD) (**J**), and consecutive dry days (CDD) (**K**) in Midwest Brazil from 1979 to 2019. Large circles indicate statistical significance at the 5% level and small circles are not significant.

3.1.2. Decadal Variability

A comparison between the total precipitation (PRCPTOT) over the past four decades indicated no change in PRCPTOT throughout the Midwest as all four decades showed a constant average amount of ~1500 mm year^{-1} (Figure 3F). However, precipitation intensity and frequency have increased during the last two decades, as indicated by the mean of the maximum daily precipitation concerning Rx1day, Rx5day, and R95p (Figure 3). Similarly, the mean number of days of R20mm and R50mm increased during the last two decades. The PDF of R50mm indicated an increase of 2 days per decade (Figure 3C), and the PDFs of the

Rx1day and Rx5day indicated an increase of 8.44 mm and 12 mm per decade (Figure 3D,E), respectively. Precipitation intensity based on the SDII also increased during the last two decades by an average of 2.1 mm per decade (Figure 3G). The PDFs of the R95p and CDD indicated an increase of 84.5 mm per decade (Figure 3H) and 24.6 days per decade (Figure 3K), respectively, while the PDFs of the CWD indicated a decrease of 3.6 days per decade (Figure 3J). These patterns highlight that there is an increased frequency of extreme precipitation events occurring in short periods in the Brazilian Midwest. These patterns affect the interannual variability of precipitation extremes but have minimal impact the total annual precipitation.

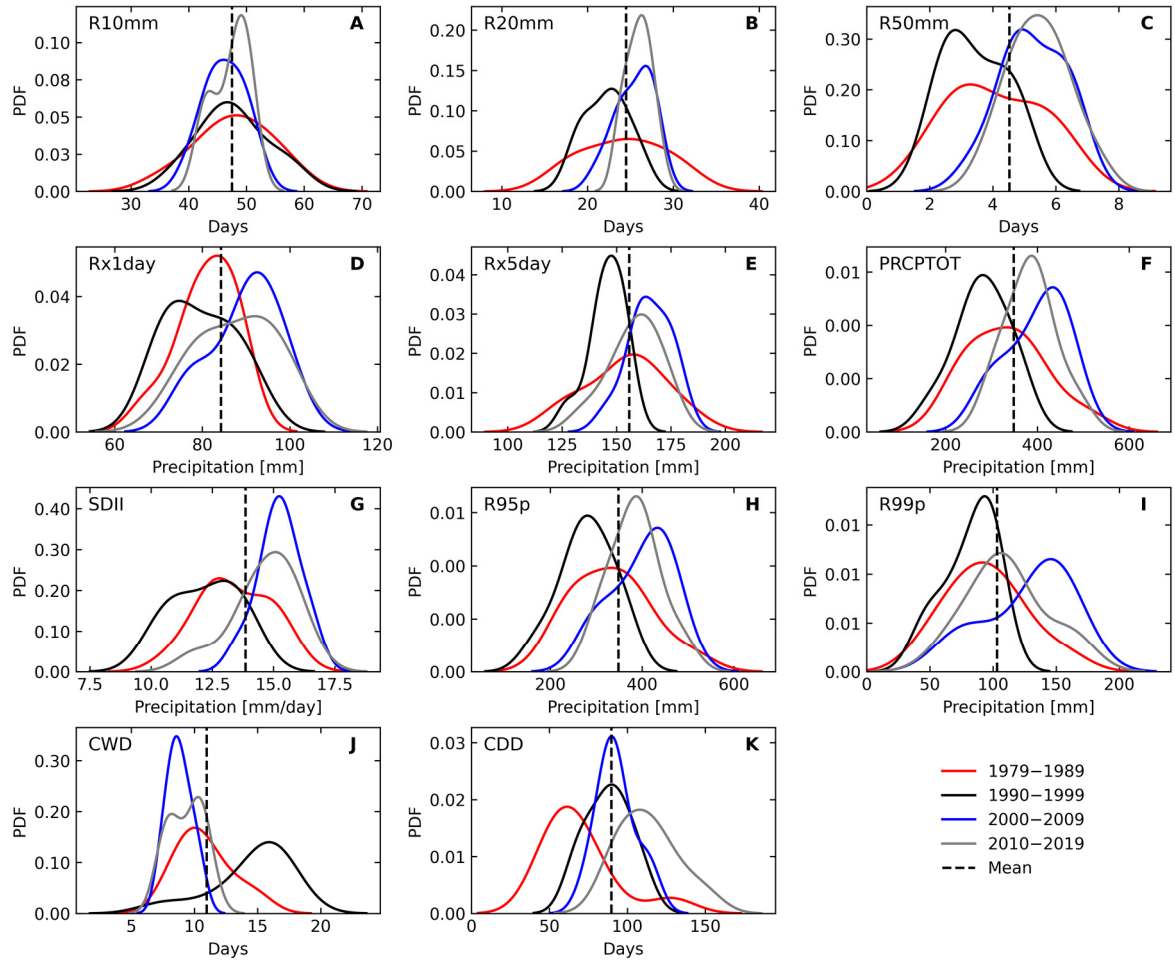

Figure 3. Probability Density Function (PDF) of the annual frequency of the number of heavy precipitation days (R10mm) (**A**), the number of very heavy precipitation days (R20mm) (**B**), the number of days above 50 mm (R50mm) (**C**), the maximum 1-day precipitation amount (Rx1day) (**D**), the maximum 5-day precipitation amount (Rx5day) (**E**), the annual total wet day precipitation (PRCPTOT) (**F**), the Simple Daily Intensity Index (SDII) (**G**), the precipitation on very wet days (R95p) (**H**), the precipitation on extremely wet days (R99p) (**I**), the Consecutive Wet Days (CWD) (**J**), and the Consecutive Dry Days (CDD) (**K**) for the Brazilian Midwest from 1979 to 2019.

3.1.3. Precipitation Extremes and SST Anomalies

Many precipitation extreme indices had significant correlations with SST anomalies across the Midwest region, which ranged from weak (0.20 to 0.39) to moderate (0.40 to 0.69) (Figure 4). In the Amazon (AMZ), R10mm had a moderate negative correlation with both TSAI and TNAI, while the CWD had a moderate correlation with TSAI. On the other hand, the frequency of extremely wet days, R99p, had a moderate negative correlation with ONI, Nino 3, Nino 4, and Nino 3.4, while the Rx1day index had a moderate correlation

with Nino 4. In the Brazilian Savanna (BSV), R10mm, CDD, and PRCPTOT had moderate negative correlations with TSAI, while R50mm, Rx1day, SDII, and R95p had moderate positive correlations with TNAI. In the Pantanal (PAN), R50mm and R95p had moderate positive correlations with TSAI, while SDII had a positive correlation with TSAI and TNAI. In the Atlantic Forest (ATF), R50mm, Rx1day, Rx5day, SDII, R95p, and R99p had moderate positive correlations with TNAI, while the R10mm and R20mm indices had moderate positive correlations with Nino 1 + 2, and PRCPTOT with Nino 3 and Nino 1 + 2. On the other hand, the CDD in the Atlantic Forest (AFT) region had a moderate negative correlation with ONI, Nino 3, and Nino 3.4.

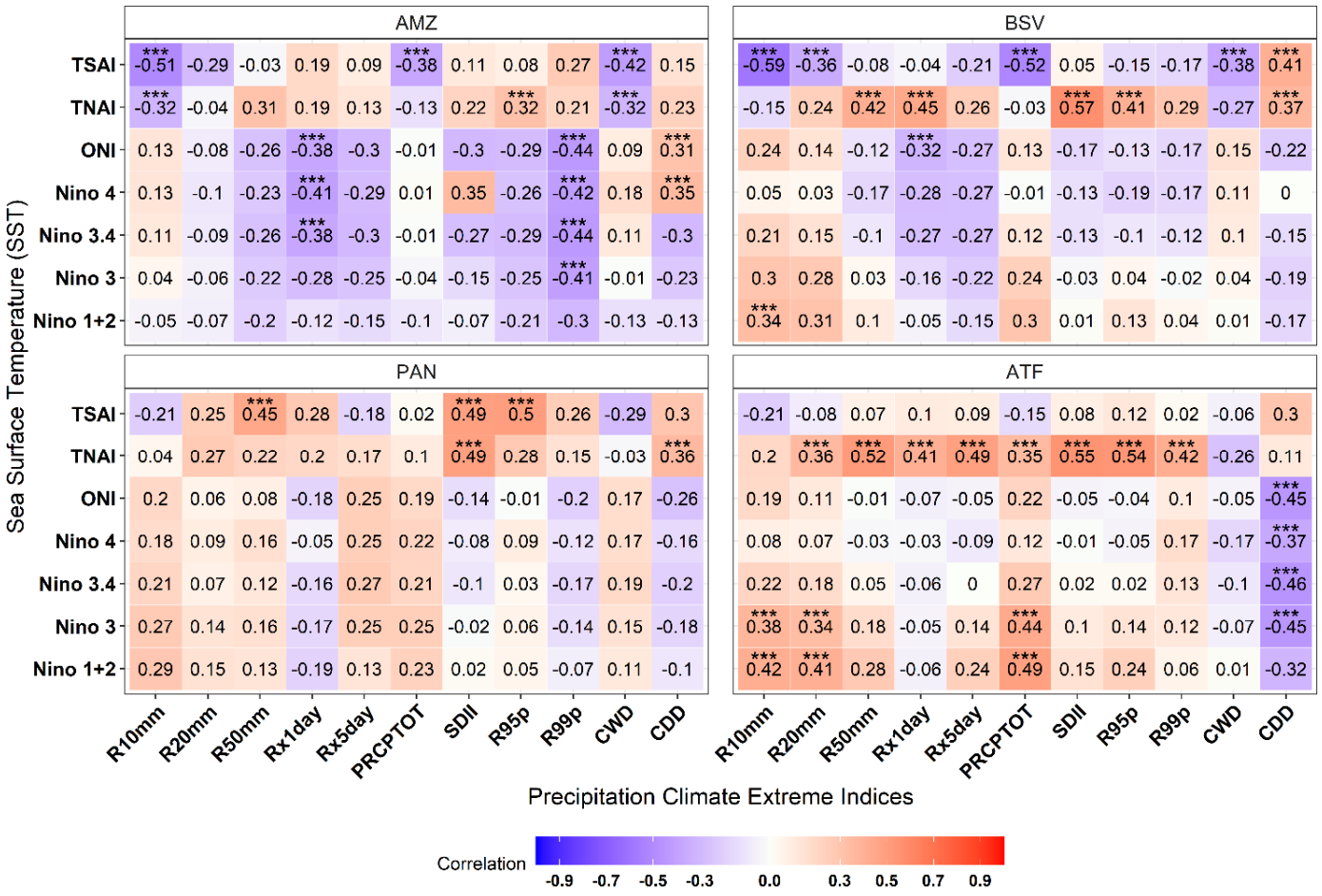

Figure 4. Pearson's correlation coefficients of Sea Surface Temperature (SST) anomalies including TSAI, TNAI, ONI, Nino 1 + 2, 3, 3.4, and 4 with precipitation extreme indices in the Amazon (AMZ), Brazilian Savanna (BSV), Pantanal (PAN), and Atlantic Forest (ATF) in the Brazilian Midwest from 1979 to 2019. Cells with *** indicate p-value < 0.05.

3.2. Temperature Extremes

3.2.1. Spatiotemporal Variability

A significant warming pattern was dominant across the Brazilian Midwest, along with a clear increase in daily temperature and a decrease in temperature on cold days and nights. TXx, TX90p, DTR, TN90p, TXn, TNx, and WSDI had a positive trend, while TX10p and TN10p had a negative trend. The Warmest Day index (TXx) had a positive trend in all study sites, except in Matupá (ID 20) and Canarana (ID 3), which are in the northern Brazilian Midwest (Figure 5A). The highest positive trend of TXx was observed in Cláudia (ID 19; 0.14 °C year^{-1}). The Warmest Night (TNx) had a positive trend in 46% of the sites, with the highest value in Corumbá (ID 22; 0.08 °C year^{-1}; Figure 5B). The Coldest Day (TXn) had a positive trend in 54% of the sites, with the highest value in Nova Xavantina

(ID 12; 0.12 °C year^{-1}; Figure 5C). The Coldest Night (TNn) had a positive trend in 50% of the sites, with the highest value in Canarana (ID 3; 0.18 °C year^{-1}; Figure 5D).

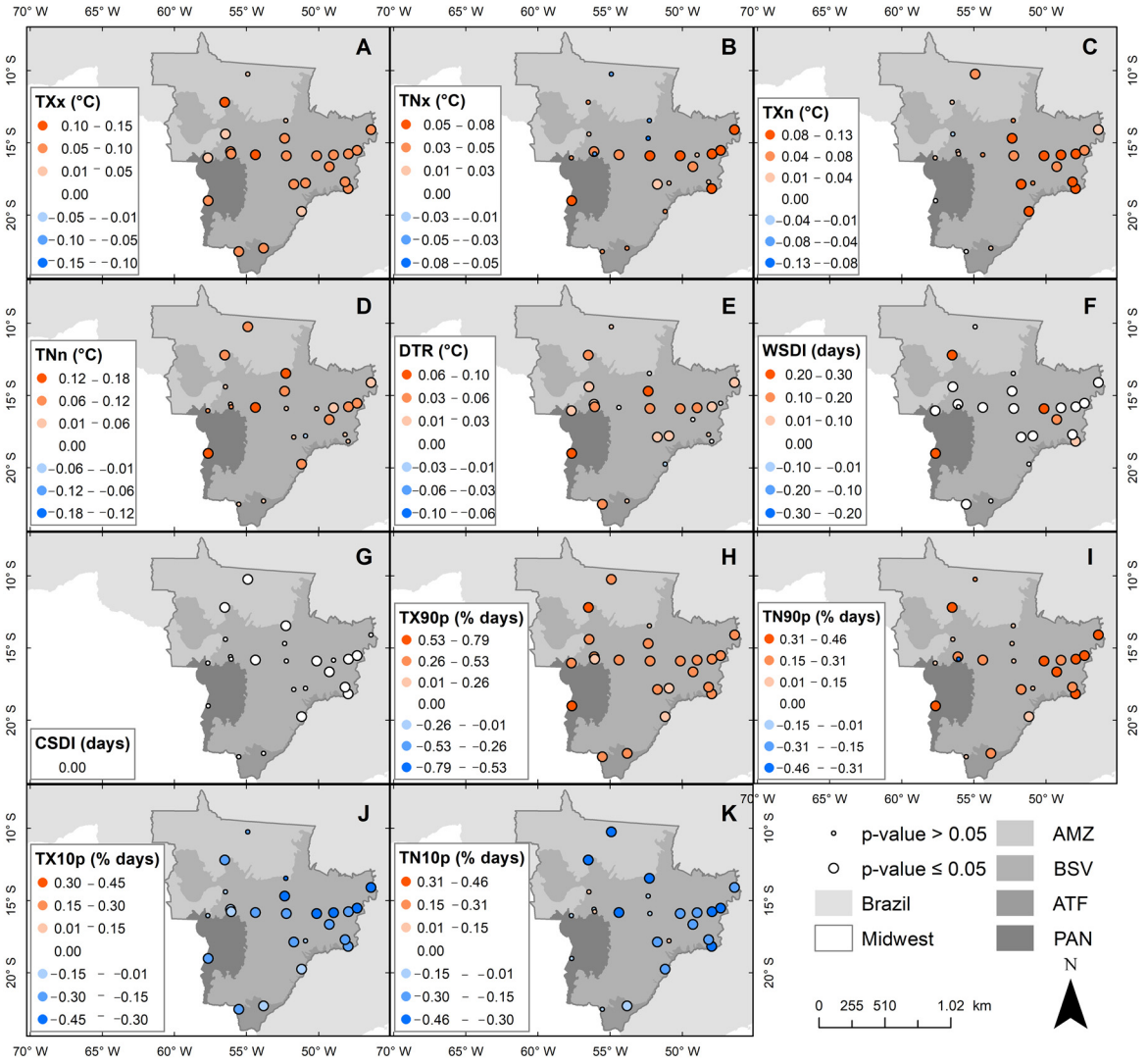

Figure 5. Spatial distribution of trends for Warmest Day (TXx) (**A**), Warmest Night (TNx) (**B**), Coldest Day (TXn) (**C**), Coldest Night (TNn) (**D**), Diurnal Temperature Range (DTR) (**E**), Warm spell duration (WSDI) (**F**), Cold spell duration (CSDI) (**G**), Warm Days (TX90p) (**H**), Warm Nights (TN90p) (**I**), Cool Days (TX10p) (**J**), and Cool Nights (TN10p) (**K**) in the Brazilian Midwest from 1979 to 2019. The bluish-colored dots refer to the range of positive trends, while the reddish-colored ones refer to that of negative trends.

The Diurnal Temperature Range (DTR) had a positive trend in 63% of the sites, with the highest value in Nova Xavantina (ID 12; 0.09 °C year^{-1}) (Figure 5E). It is noteworthy that the trend of DTR is directly related to the variability of the highest and lowest annual maximum and minimum temperatures. The warm spell duration index (WSDI) had a positive trend in 21% of the sites, with the highest value in Corumbá (0.30 day year^{-1}) (Figure 5F). On the other hand, the Cold Spell Duration Index (CSDI) had no trend (Figure 5G).

The warm days (TX90p) had a positive trend in all sites, except Canarana (ID 3; Figure 5H), with the highest value in Cláudia (ID 19; 0.79% year^{-1}). The warm nights (TN90p) had a positive trend in 63% of the sites, with the highest value in Corumbá (ID 22; 0.46% year^{-1}; Figure 5I). The cool days (TX10p) and cool nights (TN10p) had negative trends in 63% and 79% of the sites, respectively (Figure 5J,K), with the highest negative

trends of the TX10p and TN10p in Nova Xavantina (ID 12; −0.45% year^{-1}) and Cláudia (ID 19; −0.46% year^{-1}), respectively.

3.2.2. Decadal Variability

The warming trend in temperature was clear (i.e., accelerated) during the last decade (i.e., 2010–2019) compared with the long-term average of all temperature extreme indices (Figure 6). The Probability Density Functions (PDFs) indicated changes in the averages and frequency of the temperature extreme indices. The decadal mean of the TXx, TXn, TNx, and TNn increased by an average of 3.0 °C, 3.14 °C, 0.65 °C, and 4.56 °C per decade from 1979–1999 to 2000–2019 (Figure 6A–D), respectively. The cool days (TX10p) and cool nights (TN10p) decreased by an average of 6.61 days and 7.65 days from 1979–1989 to 2010–2019 (Figure 6J,K), respectively, while warm days (TX90p) and warm nights (TN90p) increased by an average of 14.79 and 11.07 days (Figure 6H,I), respectively.

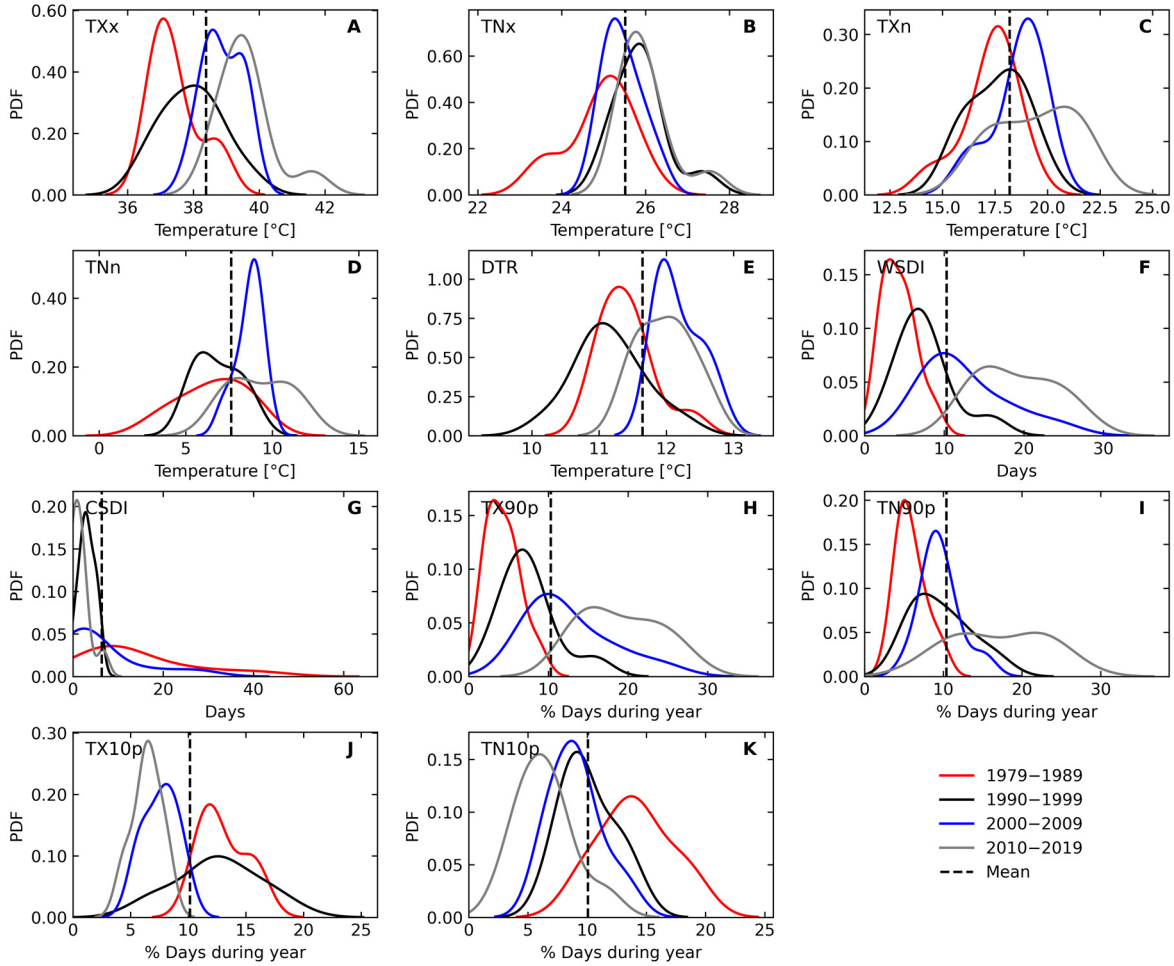

Figure 6. Probability density function (PDF) of the annual frequency of Warmest Day (TXx) (**A**), Warmest Night (TNx) (**B**), Coldest Day (TXn) (**C**), Coldest Night (TNn) (**D**), Diurnal Temperature Range (DTR) (**E**), Warm spell duration (WSDI) (**F**), Cold spell duration (CSDI) (**G**), Warm Days (TX90p) (**H**), Warm Nights (TN90p) (**I**), Cool Days (TX10p) (**J**), and Cool Nights (TN10p) (**K**) in the Brazilian Midwest from 1979 to 2019.

3.2.3. Temperature Extremes and SST Anomalies

The temperature extreme indices were significantly correlated with Pacific and Atlantic SST anomalies ranging from weak (0.20 to 0.39) to moderate (0.40 to 0.69) (Figure 7). In the Amazon (AMZ), warmest night (TNx), coldest night (TNn), and warm nights (TN90p) had moderate positive correlations with Nino 4, while warmest day (TXx) and

warm days (TX90p) had moderate positive correlations with TSAI and TNAI, and the Diurnal Temperature Range (DTR) and Warm Spell Duration (WSDI) had moderate positive correlations with TNAI. In the Brazilian Savanna (SBV), the DTR had a moderate positive correlation with TSAI and TNAI; TNx, WSDI, and TX90p had moderate positive correlations with TSAI; and Warm Nights (TN90p) had a moderate positive correlation with TSAI and Nino 4. In the Pantanal (PAN), Warmest Day (TXx), Warmest Night (TNx), and Warm Days (TX90p) had a moderately positive correlation with TNAI, and the Diurnal Temperature Range (DTR) with TSAI and TNAI. In the Atlantic Forest (ATF), Coldest Night (TNn) had a moderately positive correlation with the TNAI.

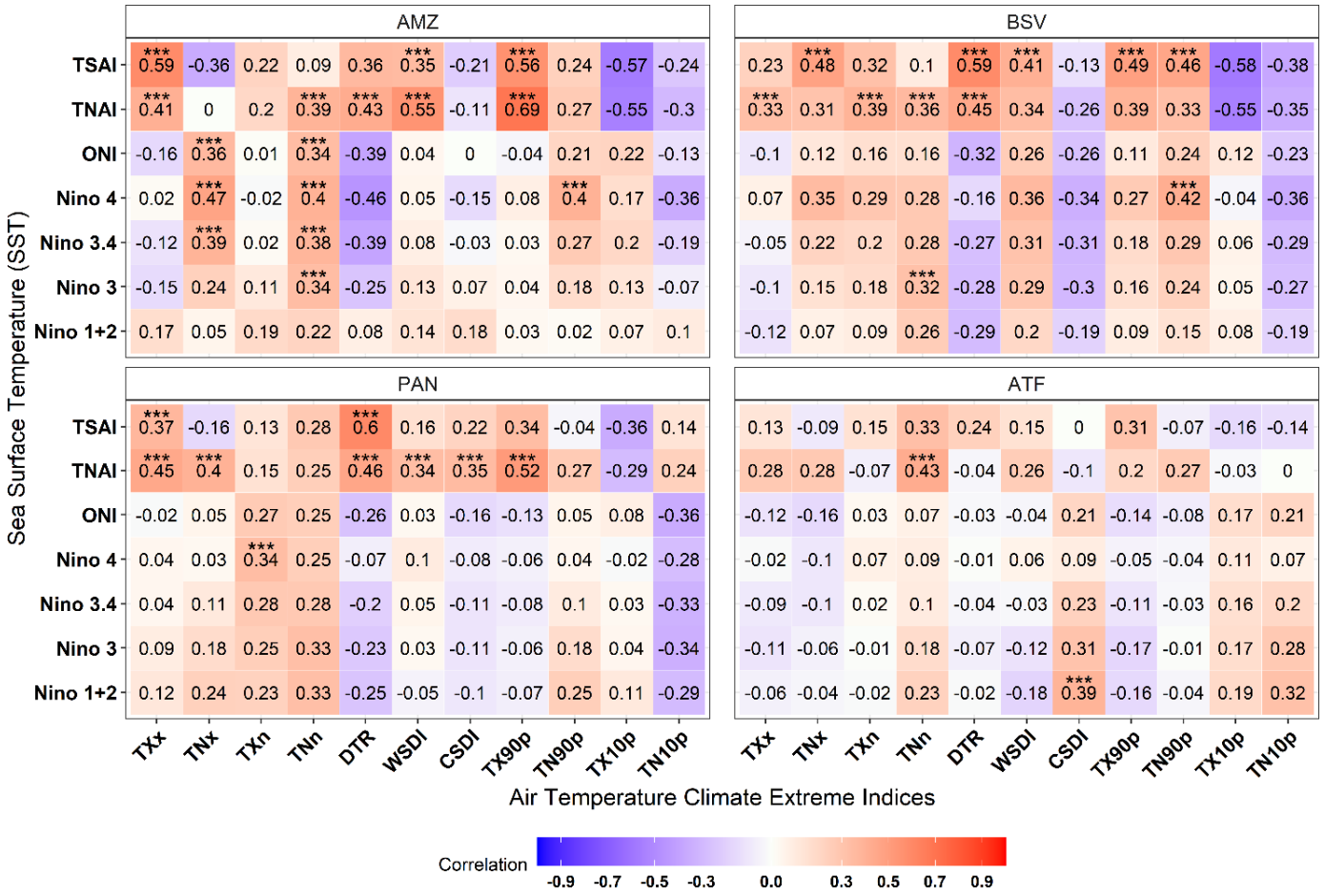

Figure 7. Pearson's correlation coefficients of Sea Surface Temperature (SST) anomalies with air temperature climate extreme indices in the Amazon (AMZ), Brazilian Savanna (BSV), Pantanal (PAN), and Atlantic Forest (ATF) in the Brazilian Midwest from 1979 to 2019. Cells with *** indicate p-value < 0.05.

4. Discussion

4.1. Precipitation and Temperature Extremes Trends

There were no long-term changes (i.e., trend) in the annual total precipitation amounts throughout the entire period of study (i.e., 1979–2019). However, the changes in the identified precipitation extremes showed that the same annual precipitation amounts have been increasingly occurring within shorter periods rather than spread through the year. The precipitation extreme indices categorically allowed for the depiction of three main characteristics: intensity/severity, frequency, and duration in the Brazilian Midwest. This behavior of the precipitation extremes has been similarly portrayed in the findings of the IPCC AR6 [2,4]. The Brazilian Midwest region evaluated in this study geographically overlaps with predefined IPCC regions for South America, including Southeastern South

America (SES), Northeastern South America (NES), and South America Monsoon (SAM) [2]. The IPCC AR6 similarly indicated that there have not been any observed changes in the mean precipitation amount, but precipitation events have intensified. In this study, it has been shown that the Amazon region experienced increased intensities in terms of the amounts that fall within 1 day, 5 days, during rainy days, or those with 95 percentile and 99 percentile exceedance probabilities as indicated by the Rx1day, Rx5day, SDII, R95p, R99p, and R50mm indices. On the other hand, precipitation events with relatively lower intensities (i.e., R10mm and R20mm) have been decreasing in the Brazilian Savanna, Pantanal, and Atlantic Forest. Like the observational data suggested in this study, the recent IPCC AR6 [4] also cautioned that this finding comes with low confidence, which is mainly due to the limited observational data available. Thus, we suggest that more representative data should be added to increase the confidence of these findings.

On the other hand, all the temperature extreme indices indicated increases in the severity, frequency, and, to some extent, duration of extreme events during the entire period of study (i.e., 1979–2019), with a general increased consistent warming effect across the Brazilian Midwest. All the temperature extreme indices (expect TNx and WSDI) showed that more than 50% of the stations have increased trends. The slight increase in the WSDI, with about 80% of the stations showing no change, can indicate the occurrence of heatwaves when combined with the increase in the temperature and amplitude of the maximum and minimum temperatures. Moreover, there was no spatial variability in these observed positive trends. The maximum temperature indices (TXx and TXn) and the minimum temperature indices (TNx and TNn) had more pronounced positive trends in the North (Amazon) and East (Brazilian Savanna) of the Midwest. There was also an increase in the frequency of hot days and nights (TX90p and TN90p) and heat waves (WSDI), while the frequency of cold days and nights decreased (TX10p and TN10p). The IPCC AR6 indicated similar findings (likely with high confidence) of a significant increase (and decrease) in the frequency and intensity of heat extremes (and cold extremes) in the SAM, NES, and SES regions of the defined IPCC sub-regions [2].

The changes in the pattern of precipitation extremes in the region may be due to the increase in air temperature, which, in turn, can allow for the enhancement of large-scale convective activities that bring/transport moisture from other locations [37–39]. The increased frequency and intensity of hot extremes can be associated with the persistent changes in land use and land cover [40]. Therefore, there was an increase in the thermal amplitude (DTR), which can be related to different climatic factors, such as topography, vegetation, and atmospheric systems [7]. The replacement of natural cover by deforestation or vegetation burning modifies the pattern of energy and water exchange [41] as the natural cover regulates surface temperature and humidity [42]. The reduction in natural biomass also implies an increase in sensible heat with which to heat the surface and a decrease in the latent heat of surface evapotranspiration [43,44]. The change in these energy and water exchange patterns modifies the boundary layer pattern and influences moisture convection and cloud properties and formation [45]. Decreased (or minimal to no change in) precipitation when combined with increased surface temperature can lead to an increased atmospheric water demand, making drought episodes more severe and widespread [46]. Urbanization is another important factor that can modify regional climates and directly influence the variability of the minimum temperature. Residual heat stored in building structures is released during the night and induces warmer night conditions (TN90p) [47]; consequently, the regional climate pattern is altered [48,49].

The implications of these observed trends in precipitation and temperature extremes for human systems and ecosystems can be devastating, as they occur concurrently and, consequently, can result in multiple cascading impacts. For example, if the current positive trends in the frequency and intensity of precipitation extremes persist in the future without significant mitigation and adaptation efforts, heavy precipitation can occur, which can lead to pluvial flooding, landslides, and rockfalls. These impacts or hazards have been positively reported across several subregions in South America including SES, NES, and

SAM [50]. On the other hand, increased dry spells, as indicated by the CDD index, can lead to increased aridity; more frequent and extended drought (mereological) events leading to a cascade of hydrological, agricultural, and ecological droughts; and conditions that trigger wildfires. Extreme heat can also impact human health, including by increasing mortality and the rates of the emergence of disease; increasing the demand for energy; and affecting urban planning [50]

4.2. Precipitation and Temperature Extremes and SST Anomalies

The importance of evaluating the relationships between SST anomalies and climate extremes arises from the need to provide accurate predictions of climate impact drivers (heatwaves, froes, floods, and droughts), which are important to allow for the evaluation of the risks to human societies and ecosystems. While there are several well-established SST anomalies, their effects (teleconnection) or abilities to predict temperature and climate extremes can vary for a number of reasons. In this study, it appeared that four Atlantic and Pacific SST anomaly indices, namely, TNAI, TSAI, Nino 4, and ONI, had negative and positive influences on precipitation and temperature (minimum and maximum), respectively, in Amazonia. During El Niño events, the pattern of atmospheric circulation changes due to the weakening of the trade winds over the Pacific. These changes in atmospheric circulation induce the occurrence of tropical convection over the central and eastern Pacific region, which can consequently alter the patterns of the Walker zonal circulation cell [51]. As a result, the ascending air movements shift from east to west, while a subsident branch of the Walker cell reduces the intensity of the ascending branch that occurs over the Amazon region. Under these conditions, convection weakens in the Amazon region and, consequently, decreases precipitation and increases temperatures in this region. [52].

The impacts of the precipitation deficit may also be related to the occurrence of different types of El Niño, such as Canonical and Modoki [53]. While Canonical El Niño propagates positive SST anomalies westward from the coast of South America, El Niño Modoki generates the largest positive SST anomalies in the Central Equatorial Pacific region [13]. These El Niño events can affect much of Tropical South America during the summer (DJF) with different intensities [54].

El Niño events increase sensible and latent heat fluxes from the ocean to the atmosphere [51], increase convective activity, and cause the mean temperature of the tropical troposphere to be up to 1 °C higher than in La Niña episodes [55]. In addition, the lower tropospheric temperature also increases the temperature in El Niño years due to sensible heat transfer to the air, which reinforces conditions of a positive horizontal temperature gradient in the tropics and extratropical regions and intensifies the subtropical jet current [51]. On the other hand, the intensification and location of the subtropical jet is also associated with the intensification of the meridional circulation of the Hadley cell in El Niño episodes, reinforcing the conditions of the Mesoscale Convective Systems (MCS), which can favor precipitation extremes [55,56].

Pacific SST anomalies and extreme precipitation rates had little or no relationship in the Brazilian Savanna and Pantanal. On the other hand, the anomalies in the North and South Atlantic sector (TNAI and TSAI) had positive influences on the pattern of precipitation extremes. Precipitation in the Brazilian Savanna and Pantanal is modulated by equatorial fronts coming from the Amazon, by the actions of the South American Monsoon System (SAMS), and by the South Atlantic Convergence Zone (SACZ) [57]. As part of the dynamics of SAMS, large volumes of water vapor emerge from the Amazon in the summer, transporting most of the precipitation to the southern region. The relationships between the positive anomalies of the TNAI and precipitation extremes (droughts) may have occurred due to changes in the intensity and location of the low-level subtropical jet, which may affect the evapotranspiration from the Amazon to the Brazilian Savanna and Pantanal [11,58]. Pacific SST anomalies (Niño 3) were also associated with increased air temperature in the Brazilian Savanna. However, the variability of the Atlantic Dipole (TNAI and TSAI) provided an increase in air temperature due to a greater increase trend

of the maximum temperature compared to the minimum temperature, causing a greater thermal range (DTR). The positive relationships between the Atlantic SST anomalies with the maximum and minimum temperature indices in the Pantanal indicated that the increase in the Atlantic SST influenced the greater occurrence of heat waves (WSDI) and cold waves (CSDI) as well as the temperature range.

In the Atlantic Forest, Pacific SST anomalies positively influenced the intensity of precipitation events. El Niño and La Niña events increased and decreased rainfall totals during the year, respectively. On the other hand, only the TNAI was related to precipitation and air temperature; specifically, it was positively related to the variability of precipitation in the region, and negatively related to the minimum air temperature. Also in this region, Niño 1 + 2 favored the occurrence of cold waves.

4.3. Limitations and Future Studies

This study highlighted important precipitation and temperature extremes across different sub-regions in the Brazilian Midwest. However, the number and distribution of stations used throughout the Pantanal region (i.e., three stations) should not be considered as fully representative of its spatial variability. This limitation is due to known factors. Specifically, the Brazilian Midwest has a low density of weather stations in most areas, and several stations have a great number of missing data [59]. The installation and maintenance of meteorological stations face major accessibility challenges that affect people and communication in this region. For example, the Amazon Forest is tall and dense, and the Pantanal is the largest floodplain in the world. The Amazon region is populated with a mosaic of indigenous land and conservation units. Presently, large parts of these regions can only be accessed by boat or plane. Cities in the northern region of the state of Mato Grosso (south of the Amazon) have been recently developed, i.e., the late 1970s [60], and there are no urban centers in the middle of the Pantanal. Urban centers (i.e., cities) are located on the edge of the Pantanal due to the difficulty of accessing this region, especially during the flood period. To date, there are few meteorological stations in the north of Mato Grosso and in the Pantanal. Thus, there is no long-term meteorological dataset that fully covers these regions. This type of problem did not occur in the Brazilian Savannah due to its ease of access with respect to the installation of meteorological stations because of the characteristics of this region's vegetation.

The limited number of stations in the middle of the Amazon and in the Pantanal, with two meteorological stations in the Amazon and three in the Pantanal, can poses challenges with respect to the generalization of the results in these biomes. The importance of this study arises from the need to highlight the observed climate extremes (at least) at the available stations (without generalizing them to these two regions) due to their related economic contribution to Brazil's GDP.

On the other hand, it should also be highlighted that the climatology of the Brazilian Midwest is controlled by meso- and macro-scale events. The climate of the Pantanal is hyper-seasonal tropical savannah with two well-defined water seasons: a dry one that occurs during the winter months in the southern region, and a wet one that occurs during the summer [11,39]. Due to these large-scale events, changes in the microclimate have minimal influence on regional climate variability due to surface homogeneity in terms of water and vegetation. Thus, the climate of the Pantanal is influenced by tropical systems of medium and large scales, such as the continental action of the semi-permanent high of the South Atlantic (in winter), which causes the dry period, and systems such as the High of Bolivia, the South Atlantic Convergence Zone (SACZ), and the Humidity Convergence Zone, among others. Therefore, the meteorological stations in the study area may not be geographically representative. In the future, we intend to highlight any differences or agreement between ground-based meteorological observations compared to those from reanalysis datasets such as ERA5 of the European Center for Medium-Range Weather Forecasts (ECMWF).

5. Conclusions

This study indicated that there is minimal to no interannual variability in the precipitation amounts in the analyzed region. However, it was observed that the frequency and intensity of precipitation extremes increased across many parts of the Brazilian Midwest. The total annual precipitation remained constant throughout the period from 1979 to 2019, while there was an increased trend in intense precipitation events and dry spells during the past two decades since 2000. On the other hand, there was a consistent warming trend since 1979 with an increasing trend in the hot temperature extremes and a declining trend in cold extremes across the Brazilian Midwest. In other words, the intensity of daily precipitation and hot days and nights tended to increase, while that of cold days and nights tended to decrease. In addition, there was a large variation in the difference between the maximum and minimum temperature. These trends in precipitation and temperature extremes were predicted using certain sea surface temperature (SST) anomaly indices. The Equatorial Pacific and Atlantic SST anomalies influenced the decrease in the precipitation extreme indices and the increase in the air temperature extreme indices across the Amazon. However, there was a predominance of Atlantic SST anomalies (TSAI and TNAI) in the Brazilian Savanna and Pantanal, which influenced the increase in the precipitation and air temperature extreme indices. In addition, the Pacific SST anomalies (Niño 1 + 2 and Niño 3) influenced the increase in precipitation intensity in the Atlantic Forest.

These findings can help improve our understanding of the variability in the precipitation and temperature extremes in the Brazilian Midwest and their relationship with Pacific and Atlantic SST. The comprehension and prediction of the regional and local scale impacts of climate change on key economic activities in this region is important in order to provide guidance for many entities, including regional climate centers, decision-makers, and resource managers, to develop mitigation and adaptation policies and practices to ensure the health and safety of human societies and ecosystems. Although this study highlights trends in precipitation and temperature extremes in the Brazilian Midwest region, further studies must be carried out to identify these trends in areas not covered by the weather stations used in this study.

Author Contributions: Conceptualization, M.S.B., N.G.M., and L.O.F.d.S.; methodology, L.O.F.d.S., M.S.B., N.G.M., C.A.S.Q., and A.L.R.; software, L.O.F.d.S.; formal analysis, L.O.F.d.S., M.S.B., and N.G.M.; investigation, L.O.F.d.S., N.G.M., I.O.I., N.L.N., C.A.S.Q., and A.L.R.; resources, N.G.M., M.S.B., and H.M.E.G.; data curation, L.O.F.d.S.; writing—original draft preparation, L.O.F.d.S., N.G.M., M.S.B., H.M.E.G., and N.G.M.; writing—review and editing, L.O.F.d.S., N.G.M., M.S.B., H.M.E.G., and N.G.M.; visualization, M.S.B., N.G.M., and H.M.E.G.; supervision, N.G.M. and M.S.B.; project administration, N.G.M. and M.S.B.; funding acquisition, N.G.M., M.S.B., and H.M.E.G. All authors have read and agreed to the published version of the manuscript.

Funding: This research was partially funded by Conselho Nacional de Desenvolvimento Científico e Tecnológico (CNPq), code #407463/2016-0, #311541/2021-6 and #311907/2021-0, Fundação de Amparo à Pesquisa do Estado de Mato Grosso (FAPEMAT), code #561397/2014, Universidade Federal de Mato Grosso (UFMT), Programa de Pós-Graduação em Física Ambiental (PPGFA/IF/UFMT), Instituto Federal de Mato Grosso (IFMT), the National Science Foundation (NSF) Award Number IIA-1301346 and 1739835 and New Mexico State University.

Institutional Review Board Statement: Not applicable.

Informed Consent Statement: Not applicable.

Data Availability Statement: All data used in this work are available in the Meteorological Database for Teaching and Research (BDMEP; https://bdmep.inmet.gov.br/; accessed on 15 April 2019) from the Brazilian National Institute of Meteorology (INMET).

Acknowledgments: The authors would like to thank the Brazilian National Institute of Meteorology (INMET) to provide data to this research.

Conflicts of Interest: The authors declare no conflict of interest.

References

1. Moreira, P.S.P.; Dallacort, R.; Santos Galvanin, E.A.; Neves, R.J.; Carvalho, M.A.C.; Barbieri, J.D. Ciclo diário de variáveis meteorológicas nos biomas do estado de Mato Grosso (meteorological variables daily cycle in Mato Grosso state biomes. *Rev. Bras. Climatol.* **2015**, *17*, 173–188.
2. Castellanos, E.J.; Lemos, M.F. IPCC Sixth Assessment Report (AR6): Climate Change 2022-Impacts, Adaptation and Vulnerability: Regional Factsheet Central and South America. 2022. Available online: https://www.ipcc.ch/report/ar6/wg2/ (accessed on 3 January 2023).
3. Almagro, A.; Oliveira, P.T.S.; Nearing, M.A.; Hagemann, S. Projected Climate Change Impacts in Rainfall Erosivity over Brazil. *Sci Rep* **2017**, *7*, 8130. [CrossRef]
4. Seneviratne, S.I.; Zhang, X.; Adnan, M.; Badi, W.; Dereczynski, C.; Di Luca, A.; Vicente-Serrano, S.M.; Wehner, M.; Zhou, B. Chapter 11: Weather and Climate Extreme Events in a Changing Climate. 2021. Available online: https://www.ipcc.ch/report/ar6/wg1/downloads/report/IPCC_AR6_WGI_Chapter11.pdf/ (accessed on 3 January 2023).
5. Machado, N.G.; Biudes, M.S.; Querino, C.A.S.; Danelichen, V.H.d.M.; Velasque, M.C.S. Seasonal and Interannual Pattern of Meteorological Variables in Cuiabá, Mato Grosso State, Brazil. *Rev. Bras. Geofis.* **2015**, *33*, 477–488. [CrossRef]
6. Sein, K.K.; Chidthaisong, A.; Oo, K.L. Observed Trends and Changes in Temperature and Precipitation Extreme Indices over Myanmar. *Atmosphere* **2018**, *9*, 477. [CrossRef]
7. Ely, D.F.; Fortin, G. Trend Analysis of Extreme Thermal Indices in South Brazil (1971 to 2014). *Theor. Appl. Climatol.* **2020**, *139*, 1045–1056. [CrossRef]
8. Kim, Y.-H.; Min, S.-K.; Zhang, X.; Sillmann, J.; Sandstad, M. Evaluation of the CMIP6 Multi-Model Ensemble for Climate Extreme Indices. *Weather. Clim. Extrem.* **2020**, *29*, 100269. [CrossRef]
9. Avila-Diaz, A.; Benezoli, V.; Justino, F.; Torres, R.; Wilson, A. Assessing Current and Future Trends of Climate Extremes across Brazil Based on Reanalyses and Earth System Model Projections. *Clim. Dyn.* **2020**, *55*, 1403–1426. [CrossRef]
10. Dunn, R.J.H.; Alexander, L.V.; Donat, M.G.; Zhang, X.; Bador, M.; Herold, N.; Lippmann, T.; Allan, R.; Aguilar, E.; Barry, A.A.; et al. Development of an Updated Global Land In Situ-Based Data Set of Temperature and Precipitation Extremes: HadEX3. *J. Geophys. Res. Atmos.* **2020**, *125*, e2019JD032263. [CrossRef]
11. Thielen, D.; Schuchmann, K.-L.; Ramoni-Perazzi, P.; Marquez, M.; Rojas, W.; Quintero, J.I.; Marques, M.I. Quo Vadis Pantanal? Expected Precipitation Extremes and Drought Dynamics from Changing Sea Surface Temperature. *PLoS ONE* **2020**, *15*, e0227437. [CrossRef]
12. Cai, W.; McPhaden, M.J.; Grimm, A.M.; Rodrigues, R.R.; Taschetto, A.S.; Garreaud, R.D.; Dewitte, B.; Poveda, G.; Ham, Y.-G.; Santoso, A.; et al. Climate Impacts of the El Niño–Southern Oscillation on South America. *Nat. Rev. Earth Environ.* **2020**, *1*, 215–231. [CrossRef]
13. Viegas, J.; Andreoli, R.V.; Kayano, M.T.; Candido, L.A.; de Souza, R.A.F.; Hall, D.H.; de Souza, A.C.; Garcia, S.R.; Temoteo, G.G.; Valentin, W.I.D. Caracterização dos Diferentes Tipos de El Niño e seus Impactos na América do Sul a Partir de Dados Observados e Modelados. *Rev. Bras. Meteorol.* **2019**, *34*, 43–67. [CrossRef]
14. Lin, J.; Qian, T. A New Picture of the Global Impacts of El Nino-Southern Oscillation. *Sci. Rep.* **2019**, *9*, 17543. [CrossRef]
15. Wainer, I.; Prado, L.F.; Khodri, M.; Otto-Bliesner, B. The South Atlantic Sub-Tropical Dipole Mode since the Last Deglaciation and Changes in Rainfall. *Clim. Dyn.* **2021**, *56*, 109–122. [CrossRef]
16. Costa, R.L.; Macedo de Mello Baptista, G.; Gomes, H.B.; Daniel dos Santos Silva, F.; Lins da Rocha Júnior, R.; de Araújo Salvador, M.; Herdies, D.L. Analysis of Climate Extremes Indices over Northeast Brazil from 1961 to 2014. *Weather. Clim. Extrem.* **2020**, *28*, 100254. [CrossRef]
17. Da Silva, P.E.; Santos e Silva, C.M.; Spyrides, M.H.C.; Andrade, L.d.M.B. Precipitation and Air Temperature Extremes in the Amazon and Northeast Brazil. *Int. J. Climatol.* **2019**, *39*, 579–595. [CrossRef]
18. Dereczynski, C.; Chan Chou, S.; Lyra, A.; Sondermann, M.; Regoto, P.; Tavares, P.; Chagas, D.; Gomes, J.L.; Rodrigues, D.C.; Skansi, M.d.l.M. Downscaling of Climate Extremes over South America—Part I: Model Evaluation in the Reference Climate. *Weather. Clim. Extrem.* **2020**, *29*, 100273. [CrossRef]
19. Marengo, J.A.; Camargo, C.C. Surface Air Temperature Trends in Southern Brazil for 1960–2002. *Int. J. Climatol.* **2008**, *28*, 893–904. [CrossRef]
20. Marrafon, V.H.; Reboita, M.S. Características da precipitação na América do Sul reveladas através de índices climáticos. *Rev. Bras. Climatol.* **2020**, *26*, 663–676. [CrossRef]
21. dos Santos, C.A.C.; de Brito, J.I.B.; Júnior, C.H.F.d.S.; Dantas, L.G. Trends in precipitation extremes over the Northern part of Brazil from ERA40 dataset. *Rev. Bras. Geogr. Física* **2012**, *5*, 836–851. [CrossRef]
22. Alvares, C.A.; Stape, J.L.; Sentelhas, P.C.; De Moraes Gonçalves, J.L.; Sparovek, G. Köppen's Climate Classification Map for Brazil. *Meteorol. Z.* **2013**, *22*, 711–728. [CrossRef]
23. INMET Meteorological Database for Teaching and Research (BDMEP). Available online: https://bdmep.inmet.gov.br/ (accessed on 5 February 2023).
24. WMO. *Manual on the Global Observing System, Volume I, Global Aspects*; WMO: Geneva, Switzerland, 2013; ISBN 978-92-63-10544-8.
25. Huang, B.; Thorne, P.W.; Banzon, V.F.; Boyer, T.; Chepurin, G.; Lawrimore, J.H.; Menne, M.J.; Smith, T.M.; Vose, R.S.; Zhang, H.-M. Extended Reconstructed Sea Surface Temperature, Version 5 (ERSSTv5): Upgrades, Validations, and Intercomparisons. *J. Clim.* **2017**, *30*, 8179–8205. [CrossRef]

26. World Climate Research Programme (WCRP). Available online: https://www.wcrp-climate.org/ (accessed on 5 February 2023).
27. Zhang, X.; Yang, F. *RClimDex (1.0) User Manual*; Climate Research Branch Environment Canada: Downsview, ON, Canada, 2004.
28. Climdex Indices. Available online: https://www.climdex.org/learn/indices/ (accessed on 5 February 2023).
29. Alexander, L.V.; Zhang, X.; Peterson, T.C.; Caesar, J.; Gleason, B.; Klein Tank, A.M.G.; Haylock, M.; Collins, D.; Trewin, B.; Rahimzadeh, F.; et al. Global Observed Changes in Daily Climate Extremes of Temperature and Precipitation. *J. Geophys. Res. Atmos.* **2006**, *111*, D05109. [CrossRef]
30. Sun, Q.; Zhang, X.; Zwiers, F.; Westra, S.; Alexander, L.V. A Global, Continental, and Regional Analysis of Changes in Extreme Precipitation. *J. Clim.* **2021**, *34*, 243–258. [CrossRef]
31. Ohlson, J.A.; Kim, S. Linear Valuation without OLS: The Theil-Sen Estimation Approach. *Rev. Account. Stud.* **2015**, *20*, 395–435. [CrossRef]
32. Hamed, K.H.; Ramachandra Rao, A. A Modified Mann-Kendall Trend Test for Autocorrelated Data. *J. Hydrol.* **1998**, *204*, 182–196. [CrossRef]
33. He, Y.-L.; Ye, X.; Huang, D.-F.; Huang, J.Z.; Zhai, J.-H. Novel Kernel Density Estimator Based on Ensemble Unbiased Cross-Validation. *Inf. Sci.* **2021**, *581*, 327–344. [CrossRef]
34. Bombardi, R.J.; Carvalho, L.M.V. de Práticas Simples em Análises Climatológicas: Uma Revisão. *Rev. Bras. Meteorol.* **2017**, *32*, 311–320. [CrossRef]
35. Liu, Y.; Cobb, K.M.; Song, H.; Li, Q.; Li, C.-Y.; Nakatsuka, T.; An, Z.; Zhou, W.; Cai, Q.; Li, J.; et al. Recent Enhancement of Central Pacific El Niño Variability Relative to Last Eight Centuries. *Nat. Commun.* **2017**, *8*, 15386. [CrossRef]
36. Bretherton, C.S.; Widmann, M.; Dymnikov, V.P.; Wallace, J.M.; Bladé, I. The Effective Number of Spatial Degrees of Freedom of a Time-Varying Field. *J. Clim.* **1999**, *12*, 1990–2009. [CrossRef]
37. Loriaux, J.M.; Lenderink, G.; Siebesma, A.P. Large-Scale Controls on Extreme Precipitation. *J. Clim.* **2017**, *30*, 955–968. [CrossRef]
38. Ruiz-Alvarez, O.; Singh, V.P.; Enciso-Medina, J.; Ontiveros-Capurata, R.E.; dos Santos, C.A.C. Observed Trends in Daily Extreme Precipitation Indices in Aguascalientes, Mexico. *Meteorol. Appl.* **2020**, *27*, e1838. [CrossRef]
39. Biudes, M.S.; Geli, H.M.E.; Vourlitis, G.L.; Machado, N.G.; Pavão, V.M.; dos Santos, L.O.F.; Querino, C.A.S. Evapotranspiration Seasonality over Tropical Ecosystems in Mato Grosso, Brazil. *Remote Sens.* **2022**, *14*, 2482. [CrossRef]
40. Hanlon, H.M.; Bernie, D.; Carigi, G.; Lowe, J.A. Future Changes to High Impact Weather in the UK. *Climatic Chang.* **2021**, *166*, 50. [CrossRef]
41. Ivo, I.O.; Biudes, M.S.; Vourlitis, G.L.; Machado, N.G.; Martim, C.C. Effect of Fires on Biophysical Parameters, Energy Balance and Evapotranspiration in a Protected Area in the Brazilian Cerrado. *Remote Sens. Appl. Soc. Environ.* **2020**, *19*, 100342. [CrossRef]
42. Biudes, M.S.; Vourlitis, G.L.; Machado, N.G.; de Arruda, P.H.Z.; Neves, G.A.R.; de Almeida Lobo, F.; Neale, C.M.U.; de Souza Nogueira, J. Patterns of Energy Exchange for Tropical Ecosystems across a Climate Gradient in Mato Grosso, Brazil. *Agric. For. Meteorol.* **2015**, *202*, 112–124. [CrossRef]
43. Barkhordarian, A.; Saatchi, S.S.; Behrangi, A.; Loikith, P.C.; Mechoso, C.R. A Recent Systematic Increase in Vapor Pressure Deficit over Tropical South America. *Sci. Rep.* **2019**, *9*, 15331. [CrossRef] [PubMed]
44. Machado, N.G.; Biudes, M.S.; Angelini, L.P.; Querino, C.A.S.; da Silva Angelini, P.C.B. Impact of Changes in Surface Cover on Energy Balance in a Tropical City by Remote Sensing: A Study Case in Brazil. *Remote Sens. Appl. Soc. Environ.* **2020**, *20*, 100373. [CrossRef]
45. Kharol, S.K.; Kaskaoutis, D.G.; Sharma, A.R.; Singh, R.P. Long-Term (1951–2007) Rainfall Trends around Six Indian Cities: Current State, Meteorological, and Urban Dynamics. *Adv. Meteorol.* **2013**, *2013*, e572954. [CrossRef]
46. Sherwood, S.; Fu, Q. A Drier Future? *Science* **2014**, *343*, 737–739. [CrossRef]
47. Kuczyński, T.; Staszczuk, A. Experimental Study of the Influence of Thermal Mass on Thermal Comfort and Cooling Energy Demand in Residential Buildings. *Energy* **2020**, *195*, 116984. [CrossRef]
48. Pires, G.F.; Abrahão, G.M.; Brumatti, L.M.; Oliveira, L.J.C.; Costa, M.H.; Liddicoat, S.; Kato, E.; Ladle, R.J. Increased Climate Risk in Brazilian Double Cropping Agriculture Systems: Implications for Land Use in Northern Brazil. *Agric. For. Meteorol.* **2016**, *228–229*, 286–298. [CrossRef]
49. Spera, S.A.; Winter, J.M.; Partridge, T.F. Brazilian Maize Yields Negatively Affected by Climate after Land Clearing. *Nat. Sustain.* **2020**, *3*, 845–852. [CrossRef]
50. Ranasinghe, R.; Ruane, A.C.; Vautard, R.; Arnell, N.; Coppola, E.; Cruz, F.A.; Dessai, S.; Saiful Islam, A.K.M.; Rahimi, M.; Carrascal, D.R. *Climate Change Information for Regional Impact and for Risk Assessment*; Cambridge University Press: Cambridge, UK, 2021.
51. Trenberth, K.E. *El Niño Southern Oscillation (ENSO). Reference Module in Earth Systems and Environmental Sciences*; Elias, S., Ed.; Elsevier: Amsterdam, The Netherlands, 2013; Volume 10, pp. 04082–04083.
52. Fonseca, M.G.; Anderson, L.O.; Arai, E.; Shimabukuro, Y.E.; Xaud, H.A.M.; Xaud, M.R.; Madani, N.; Wagner, F.H.; Aragão, L.E.O.C. Climatic and Anthropogenic Drivers of Northern Amazon Fires during the 2015–2016 El Niño Event. *Ecol. Appl.* **2017**, *27*, 2514–2527. [CrossRef]
53. Andreoli, R.V.; de Oliveira, S.S.; Kayano, M.T.; Viegas, J.; de Souza, R.A.F.; Candido, L.A. The Influence of Different El Niño Types on the South American Rainfall. *Int. J. Climatol.* **2017**, *37*, 1374–1390. [CrossRef]
54. Tedeschi, R.G.; Cavalcanti, I.F.A.; Grimm, A.M. Influences of Two Types of ENSO on South American Precipitation. *Int. J. Climatol.* **2013**, *33*, 1382–1400. [CrossRef]

55. Pereira, H.R.; Reboita, M.S.; Ambrizzi, T. Características da Atmosfera na Primavera Austral Durante o El Niño de 2015/2016. *Rev. Bras. Meteorol.* **2017**, *32*, 293–310. [CrossRef]
56. dos Santos, J.G.M.; de Campos, C.R.J.; Lima, K.C. Análise de jatos de baixos níveis associados aum sistema convectivo de mesoescala na américa do sul: Um estudo de caso. *Rev. Bras. Geof.* **2008**, *26*, 451–468. [CrossRef]
57. Liebmann, B.; Mechoso, C.R. The South American Monsoon System. In *The Global Monsoon System*; World Scientific Series on Asia-Pacific Weather and Climate; World Scientific: Singapore, 2011; Volume 5, pp. 137–157. ISBN 978-981-4343-40-4.
58. Krepper, C.M.; Zucarelli, G.V. Climatology of Water Excesses and Shortages in the La Plata Basin. *Theor. Appl. Climatol.* **2010**, *102*, 13–27. [CrossRef]
59. Xavier, A.C.; King, C.W.; Scanlon, B.R. Daily Gridded Meteorological Variables in Brazil (1980–2013). *Int. J. Climatol.* **2016**, *36*, 2644–2659. [CrossRef]
60. Nascimento, N.; West, T.A.P.; Börner, J.; Ometto, J. What Drives Intensification of Land Use at Agricultural Frontiers in the Brazilian Amazon? Evidence from a Decision Game. *Forests* **2019**, *10*, 464. [CrossRef]